

RESEARCH ARTICLE

Viral-mediated delivery of the late-infantile neuronal ceroid lipofuscinosis gene, *TPP-I* to the mouse central nervous system

RE Haskell¹, SM Hughes¹, JA Chiorini², JM Alisky¹ and BL Davidson^{1,3,4}

Program in Gene Therapy, Departments of ¹Internal Medicine, ³Neurology, ⁴Physiology & Biophysics, University of Iowa College of Medicine, Iowa City, IA, USA; ²National Institute of Dental and Craniofacial Research, National Institutes of Health, Bethesda, MD, USA

Classical late-infantile neuronal ceroid lipofuscinosis (LINCL) is caused by mutations in tripeptidyl peptidase I (TPP-I), a pepstatin-insensitive lysosomal protease, resulting in neurodegeneration, acute seizures, visual and motor dysfunction. *In vitro* studies suggest that TPP-I is secreted from cells and subsequently taken up by neighboring cells, similar to other lysosomal enzymes. As such, TPP-I is an attractive candidate for enzyme replacement or gene therapy. In the present studies, we examined the feasibility of gene transfer into mouse brain using recombinant adenovirus (Ad), feline immunodeficiency virus (FIV) and adeno-associated virus (AAV) vectors expressing TPP-I, after single injections into the striatum or cerebellum. A dual TPP-I- and β -galactosidase-expressing adenovirus vector (AdTTP-I/nls β gal) was used to distinguish transduced (β -galactosidase positive) cells from cells that endocytosed secreted TTP-I. Ten days

after striatal injection of AdTTP-I/nls β gal, β -galactosidase-positive cells were concentrated around the injection site, corpus callosum, ependyma and choroid plexus. In cerebellar injections, β -galactosidase expression was confined to the region of injection and in isolated neurons of the brainstem. Immunohistochemistry for TPP-I expression showed that TPP-I extended beyond areas of β -galactosidase activity. Immunohistochemistry for TTP-I after FIVTTP-I and AAV5TTP-I injections demonstrated TPP-I in neurons of the striatum, hippocampus and Purkinje cells. For all three vectors, TPP-I activity in brain homogenates was 3–7-fold higher than endogenous levels in the injected hemispheres. Our results indicate the feasibility of vector-mediated gene transfer of TPP-I to the CNS as a potential therapy for LINCL. Gene Therapy (2003) 10, 34–42. doi:10.1038/sj.gt.3301843

Keywords: Batten disease; CLN2; gene therapy; CNS; lysosomal storage disease

Introduction

The neuronal ceroid lipofuscinoses (NCLs) are a group of diseases related by accumulation of storage pigments in secondary lysosomes. Historically patients were classified by the ultrastructural morphology of the storage deposits and clinical course.^{1,2} One type of NCL is the classical late-infantile form, late-infantile neuronal ceroid lipofuscinosis (LINCL), also known as Jansky–Bielschowsky disease and CLN2 deficiency and pepinase deficiency.³ LINCL is an acute seizure disorder that begins between 4 and 6 years of age, with rapid deterioration in visual, motor and cognitive functioning. Lysosomal accumulations are evident by electron microscopy as curvilinear osmophilic deposits in tissue biopsies. The deposits consist predominantly of ATP synthase subunit c,⁴ a hydrophobic 75 amino acid lipoprotein normally localized in the inner mitochondrial membrane. Recently, gene mapping and functional genomics has allowed

identification of the disease allele, and classification of patients based on specific genetic lesions.⁵

Classical LINCL is caused by deficiency of the 46-kDa amino-tripeptidyl peptidase (TPP-I), a lysosomal serine protease with activity on peptides of less than 15 kDa.^{5–8} TPP-I, which traffics via the classical mannose-6-phosphate receptor mechanism, is synthesized as a glycosylated 66 kDa inactive precursor that is auto-activated at acidic pH to remove a 20 kDa propeptide.⁹ The relationship between subunit c accumulation and TPP-I deficiency is unclear, however data support a requirement for TPP-I early in the progressive enzymatic degradation of ATP synthase subunit c.^{10,11}

Current therapy for LINCL can only ameliorate the seizure disorder through conventional anti-epileptic drugs, but cannot change the natural history of the disorder. This would require correcting the underlying cause of lysosomal accumulation by delivery of TPP-I, or genes expressing it, to the brain. Like the soluble lysosomal enzymes arylsulfatase A and β -glucuronidase, TPP-I is secreted from expressing cells *in vitro*, and endocytosed into non-expressing cells.^{12–14} β -Glucuronidase and arylsulfatase A are also capable of being transported in a retrograde fashion from the site of secretion. Earlier studies in animal models of the lysosomal storage diseases metachromatic

Correspondence: BL Davidson, Roy J. Carver Professor in Internal Medicine, 200 EMRB, University of Iowa College of Medicine, Iowa City, IA 52252, USA

The first two authors contributed equally

Received 20 March 2002; accepted 2 June 2002

leukodystrophy and β -glucuronidase deficiency support the ability of directed gene expression for broadly distributed enzyme activity and correction of storage deficits.^{14–19} We hypothesize that, similarly, focal TPP-I expression in brain may result in enzyme activity beyond the zone of transduced cells.

Currently, the lack of an animal model precludes testing enzyme and/or gene therapy strategies for the CNS deficits of LINCL. However, viral vectors that direct high-level expression of TPP-I allow us to make an initial assessment of enzyme spread following CNS gene transfer with recombinant adenovirus (Ad), feline immunodeficiency virus (FIV) and adeno-associated virus type 5 (AAV5) vectors. FIV results in focal transduction when delivered to brain.^{19,20} Ad leads to local transduction but also moves along white matter tracts, such as the corpus callosum, for transduction of ependyma lining the ventricles.^{15,16} AAV5-derived vectors infect a relatively large volume within the mouse brain.^{20,21} In the current study, TPP-I wild-type mice (C57BL/6) were injected with Ad, FIV or AAV5 vectors encoding TPP-I into the striatum or cerebellum, and the levels and distribution of TPP-I assessed using immunohistochemistry and enzymatic assays.

Results

We first determined the nature of TPP-I secreted from virally transduced cells *in vitro*. A549 cells were infected with AdTPP-I, FIVTPP-I or Adnls β gal (control) and TPP-I activity in the media measured 48 h later. There was no measurable activity in supernatants, indicating that either TPP-I was not secreted or was secreted in the inactive form. As stated earlier, the unprocessed enzyme is inactive, with activation requiring removal of the 20 kDa pro-peptide by auto-activation at pH < 4.5. Incubation of harvested supernatants in citrate buffer pH 4.2 for 30 min prior to the addition of the substrate resulted in significant increases in TPP-I activity, up to 1000 times that of the control medium. Thus, secreted TPP-I was predominantly in the inactive form (Figure 1a). In contrast, TPP-I in cell lysates was active. The 100-fold difference in cell-associated TTP-1 activity between FIV- and Ad-infected cells did not correlate to greater enzyme activity in the conditioned media of AdTTP-I infected cells, suggesting that the limits of TTP-1 secretion are reached when activity approaches ~seven-fold over endogenous levels.

To determine if LINCL fibroblasts could activate exogenously derived TPP-I, a conditioned medium was

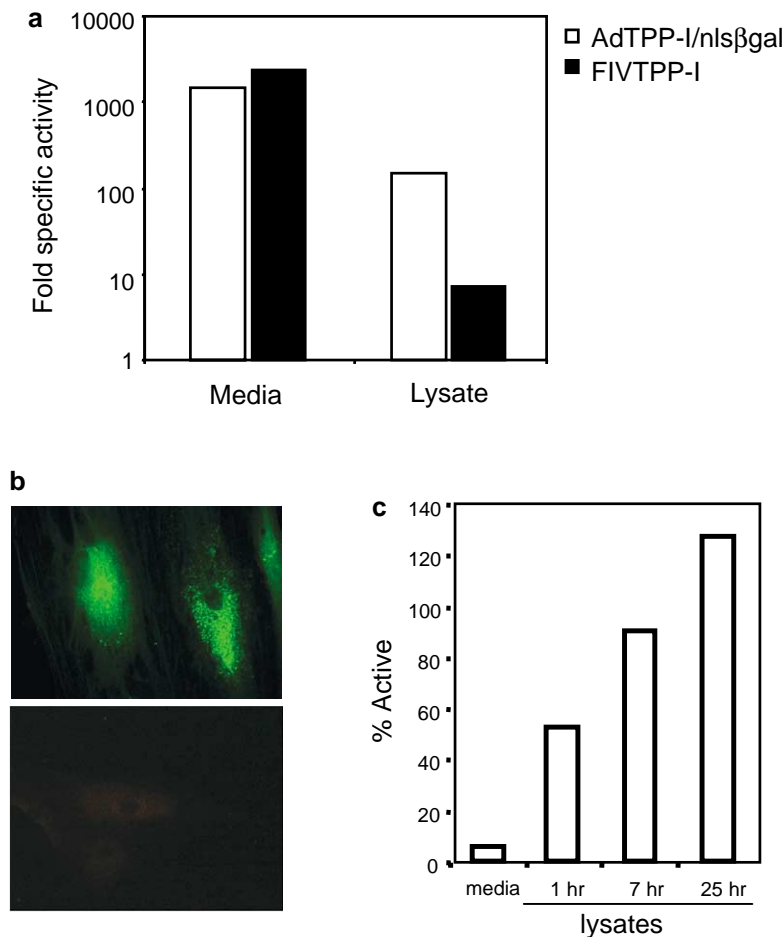


Figure 1 TPP-I activation and uptake *in vitro*. (a) TPP-I activity levels in cell lysates and media following infection of A549 cells with AdTPP-I/nls β gal or FIVTPP-I, or mock infected. Enzyme activity was normalized to mock-infected A549 cells. TPP-I in media samples was autoactivated by incubation in citrate buffer pH 4.0 for 30 min. (b) LINCL cells containing a splice junction and non-sense mutation (RMO5387), immunostained 48 h after culture in TPP-I-enriched media. Cells demonstrated TPP-I immunoreactivity (top panel), in contrast to cells cultured in control media (bottom panel). (c) TPP-I activity in LINCL fibroblast cell lysates following incubation in conditioned media from AdTPP-I/nls β gal-infected A549 cells.

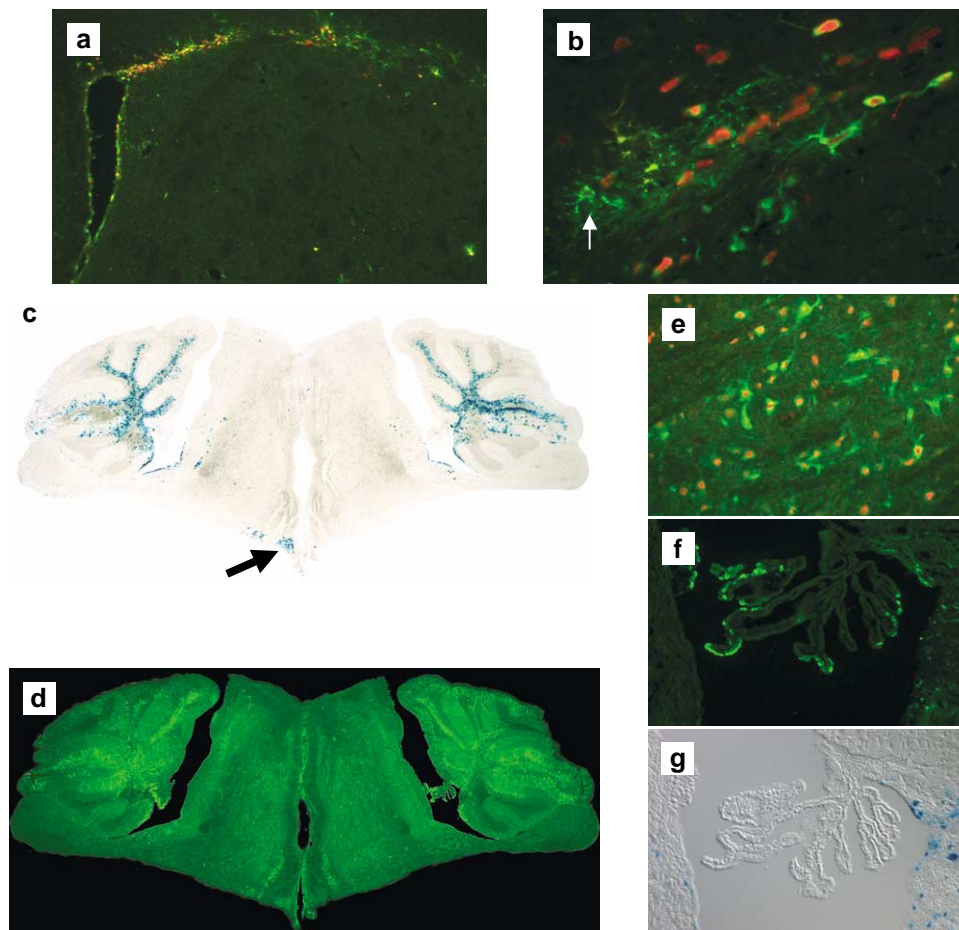


Figure 2 AdTPP-I/nls β gal expression in the cerebrum and cerebellum 10 days post-injection. (a) Photomicrograph depicting TPP-I (green) and nls β gal (red) immunoreactivity. (b) TPP-I-positive cells in the absence of β -galactosidase immunoreactivity (arrow) demonstrating uptake of TPP-I in the injected hemisphere. (c) β -Galactosidase expression in the cerebellum after injection of AdTPP-I/nls β gal into the cerebellar cortex. Note the high concentration of positive nuclei primarily in the white matter tracts of the arbor vitae and also neurons in the brain stem (arrow). (d) TPP-I immunoreactivity in the section adjacent to c. (e) Dual IHC for TPP-I (green) and NeuN (red), in the brainstem. This area from c, arrow. (f) TPP-I-positive cells in the choroid plexus from d. (g) Section adjacent to F stained for β -galactosidase expression.

prepared by infecting A549 cells with AdTPP-I/nls β gal or the control virus, Adnls β gal. AdTPP-I/nls β gal expressed TPP-I and nuclear-localized β -galactosidase (nls β gal) in the E1 and E3 regions of the adenovirus genome, respectively. TPP-I and nls β gal were expressed from the CMV or RSV promoter. LINCL fibroblasts were cultured for 48 h with conditioned or control medium from AdTPP-I/nls β gal- or Adnls β gal-infected A549 cells, respectively, and then stained for TPP-I immunoreactivity. TPP-I was localized to structures consistent with lysosomal/endosomal compartmentalization (Figure 1b). There was no immunoreactivity in cells treated with Adnls β gal-conditioned supernatant. The supernatant and cell lysates were assayed 1, 7 or 25 h after addition of media (Figure 1c). Less than 10% of the TPP-I was active in the conditioned media. After 1 h, 50% of the cell-associated TPP-I was active. By 7 and 25 h, 90% and 100% of the endocytosed TPP-I was converted to active enzyme, respectively. These data demonstrate that TPP-I-deficient cells effectively endocytosed and trafficked TPP-I to acidic compartments for activation.

The secretion of TPP-I from transduced cells after injection of 7×10^9 infectious units (i.u.) of AdTPP-I into

mouse brain was evaluated. The nuclear-targeted β -galactosidase allowed for identification of transduced cells (nls β gal⁺/TPP-I⁺) versus those that had taken up TPP-I only (TPP-I⁺/ β gal⁻). As shown in Figure 2a, IHC demonstrated TPP-I immunoreactivity in the corpus callosum, the ependyma, and the striatum following striatal injection. The majority of TPP-I-positive cells also contained β -galactosidase-positive nuclei, however some cells were clearly TPP-I⁺/ β gal⁻ (Figure 2b, arrow) indicating that secretion and uptake had occurred. In cerebella injected with AdTPP-I/nls β gal (2.9×10^9), β -galactosidase (Figure 2c) and TPP-I immunoreactivity (Figure 2d) were highest in the white matter tracts near the injection site. Radial projections and cell bodies of Bergman glia were also strongly positive for TPP-I immunoreactivity and β -galactosidase (not shown). Isolated β gal⁺ cells in the brainstem (Figure 2c, arrow) were both NeuN and TPP-I positive (Figure 2e). TPP-I immunoreactivity in these cells resulted from retrograde transport of AdTPP-I/nls β gal, rather than uptake and subsequent transport of TPP-I. TPP-I⁺/ β gal⁻ cells were particularly notable in the choroid plexus of the 4th ventricle, indicating that these non-transduced ependymal

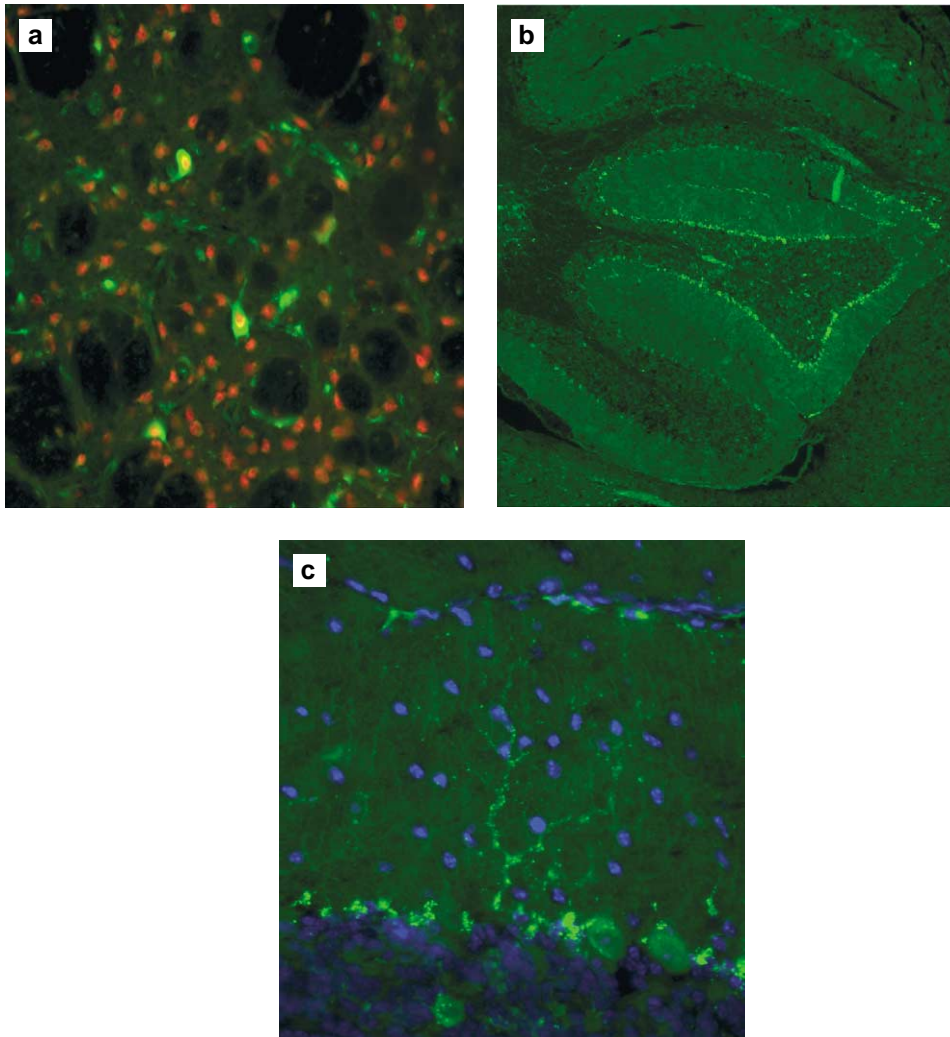


Figure 3 FIVTPP-I-mediated gene transfer to the cerebrum (a) and cerebellum (b,c). (a) TPP-I-positive, NeuN-positive cells in the striatum. (b) TPP-I immunoreactivity in Purkinje cells. (c) TPP-I staining of Purkinje cell bodies and dendrites extending into the molecular layer.

cells had endocytosed TPP-I secreted into the CSF (Figures 2f and g). Immunohistochemical analyses on naïve control brain sections were consistently negative using this rabbit polyclonal antisera (Methods).

We next tested expression from FIV- and AAV-based vectors in murine brain. In striata injected with 2.5×10^6 FIVTPP-I, TPP-I immunoreactivity was limited to the injection site and below the corpus callosum. Dual staining 10 days after injection demonstrated that the majority of TPP-I-positive cells were also positive for the neuronal marker NeuN (Figure 3a). Similar results were obtained at 16 and 33 weeks post-injection (not shown). Injections of FIVTPP-I (1×10^6 i.u) into the cerebellum resulted in TPP-I immunoreactivity in Purkinje cells and their dendrites (Figures 3b and c). For AAV5TPP-I (5×10^9 pt), we examined the distribution of TPP-I 10 weeks after striatal administration. TPP-I immunoreactivity was detected in sagittal brain slices several millimeters caudal to the injection site, especially in the hippocampus (Figure 4). This is consistent with earlier results showing that AAV5 transduces hippocampal neurons

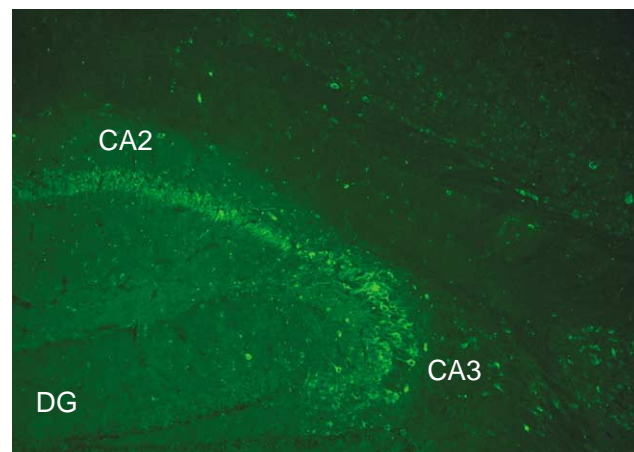


Figure 4 Expression of TPP-I 10 weeks after AAV5TPP-I injection into the cerebrum. A representative sagittal section is shown. TPP-I immunoreactivity was evident in CA2 and CA3 of the hippocampus. DG, dentate gyrus.

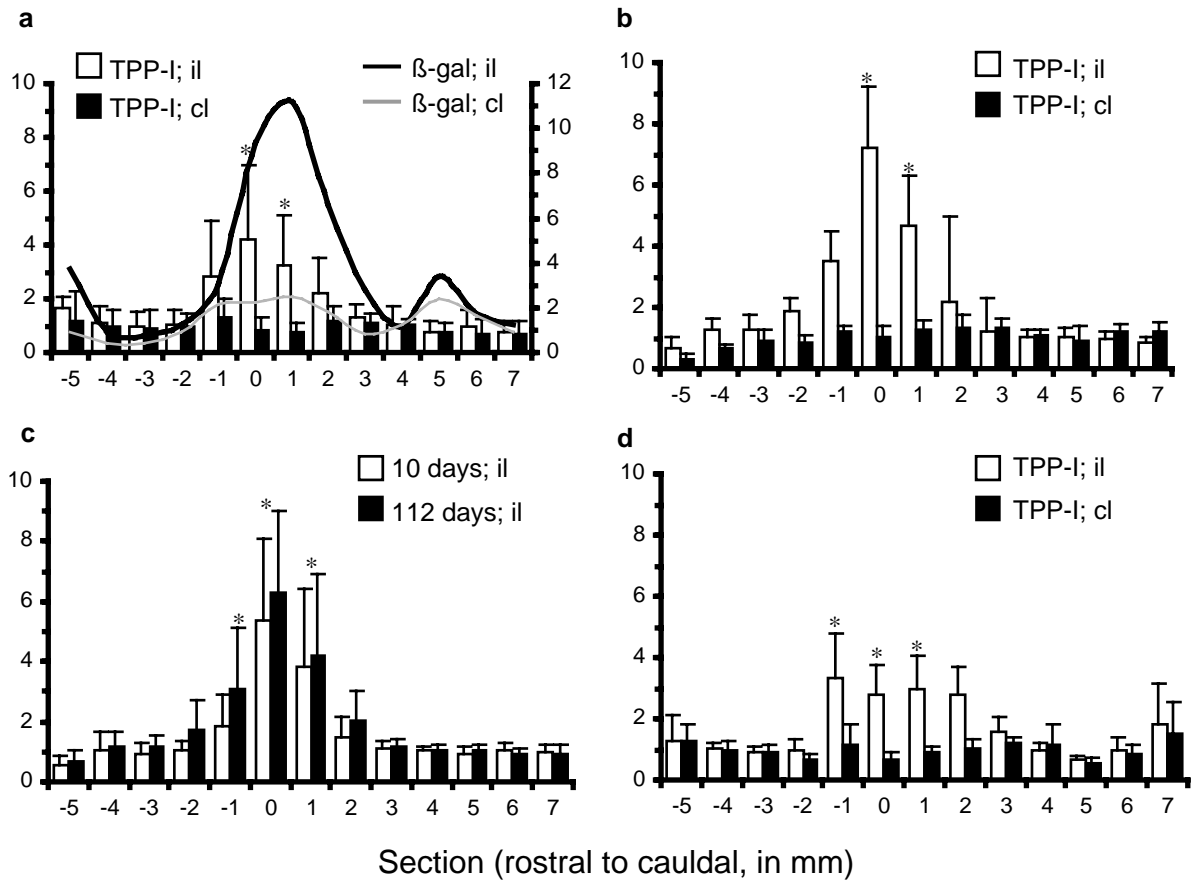


Figure 5 TPP-I enzyme activity in brain lysates. The data are represented as fold increase in activity over non-injected controls for lysates harvested rostral (–5 mm) to caudal (7 mm) of the injection site (0 position). (a) Distribution of TPP-I and β -galactosidase 10 days after AdTPP-I/nls β gal injection. TPP activity data are depicted as bar graphs (left y-axis, fluorescence units/mg protein). β -Galactosidase activity data are shown as line graphs (right y-axis, pg β -galactosidase/mg protein). Black line, injected (ipsilateral, il) hemisphere. Gray line, non-injected (contralateral, cl) hemisphere. (b) TPP-I activity 10 days after FIVTPP-I-mediated gene transfer. (c) Comparison of TPP-I activity in the injected hemispheres at 10 and 112 days following FIVTPP-I gene transfer. (d) TPP-I distribution 10 weeks after AAV5TPP-I injection into mice striata. Data represent the means \pm standard deviation. In (b)–(d), y-axis is TPP-I activity (FU/mg protein). * $P \leq 0.05$ relative to control sections in all cases.

following an intrastriatal injection (J Heth and BL Davidson, unpublished observations).

In addition to qualitative comparisons using immunohistochemistry, enzyme assays on brain lysates were done. Unlike IHC using the antibody described, endogenous levels of active TPP-I were detectable throughout the brain. At various time points after intrastriatal injection of recombinant Ad, AAV or FIV, 1-mm-thick coronal tissue slices from the entire brain were harvested and the coronal sections separated into injected (ipsilateral) and non-injected (contralateral) hemispheres. Enzyme activity in each hemisphere was independently assayed with and without pre-activation. TPP-I was in the active form as pretreatment at acidic pH did not increase levels of activity. Thus, secreted, inactive TPP-I is readily taken up and activated, or in contrast to our *in vitro* data, neural cells *in vivo* secrete TPP-I in the active form.

In mice receiving injections of 7×10^7 i.u. AdTPP-I/nls β gal, TPP-I activity was up to six times higher than endogenous levels immediate to the injection site, and significantly above endogenous levels in the surrounding 4 mm ($P < 0.05$ for 0 and 1 mm, respectively relative to Ad β gal controls). The elevation in activity was limited to

the injected hemisphere (Figure 5a). In general β -galactosidase activity correlated with TPP-I distribution, except for a consistent peak 5 mm caudal of the injection site.

FIVTPP-I injections (2.5×10^6 i.u.) also resulted in a similar-fold increase in TPP-I activity when compared to endogenous levels in control brain sections. At 10 days after injection, TPP-I activity was significantly higher than background within 2 mm of the injection site (Figure 5b; $P < 0.05$ for 0 and 1 mm respectively, relative to control). By 16 weeks (112 days), the TPP-I activity was elevated relative to the 10 day time point, with a trend toward an increased rostral distribution (Figure 5c; $P < 0.05$ for the –1, 0 and 1 mm sections, respectively relative to control). There was no further increase in enzyme levels or distribution in brains harvested and assayed 33 weeks after injection (data not shown).

Similar to AdTPP-I/nls β gal and FIVTPP-I, AAV5TPP-I (5×10^9 pt) injections resulted in TPP-I enzyme activities five-fold over background. However, and unlike brains from FIVTPP-I injected mice, AAV5TPP-I did not result in a distinct peak of TPP-I activity. We found elevated, nearly equivalent levels of enzyme 4 mm around the injection site (Figure 5d) which was significantly greater

than control treated mice ($P < 0.05$ for -1, 0 and 1 mm sections, respectively). Together, the data support that TPP-I can be expressed in brain following transduction of neurons, glia and ependyma, with spread of enzyme detectable up to 4 mm surrounding the injection site.

Discussion

Delivery of TPP-I to cells in the CNS by viral-mediated gene delivery may provide therapy for LINCL. Amelioration of the CNS deficits of this disorder would likely require widespread, rather than focal correction. Using other animal models of lysosomal storage disease as guides,^{14,15,19,22} we hypothesize that TPP-I secretion from transduced cells, followed by subsequent uptake by non-transduced cells, would lead to an extensive area of recombinant enzyme activity. In the current study we found that TPP-I expressed in brain is secreted and active, and using IHC and enzyme assay found evidence of TPP-I 2–4 mm from the injection site. While the sensitivity of our assays precludes the detection of increased enzyme expression beyond this region, we believe that the spread of enzyme may extend beyond the 2–4 mm detected. The best assessment of the extent of enzyme spread and correction will come from studies performed in animals deficient in TPP-I.

Similar to earlier work with TPP-I harvested from baculovirus-infected Sf9 cells, or overexpressing COS cells,⁹ TPP-I secreted from A549 cells was inactive. In both cases, the enzyme could be auto-activated *in vitro* at pH < 4.5, or alternatively, following endocytosis by LINCL fibroblasts and lysosomal activation. Surprisingly, we did not find evidence of inactive enzyme in brains following viral-mediated gene transfer of TPP-I. Pre-activation of tissue lysates at low pH did not enhance TPP-I activity levels, and the kinetics of each reaction were linear over the entire assay, indicating that essentially all of the TPP-I in the brain was in the active form. Our *in vitro* data support that TPP-I was secreted as the inactive 66 kDa form *in vivo* followed by immediate uptake and activation.

We were surprised to find few transduced TPP-I⁺/βgal⁻ cells given our prior experience with β-glucuronidase, and data from other published reports. This may reflect distinct differences between TPP-I and the lysosomal enzymes α-N-acetylglucosaminidase, arylsulfatase A, and β-glucuronidase with respect to their ability to spread from the site of secretion. Alternatively, it could reflect the sensitivity of our enzyme activity assay method, or the polyclonal antibody. The best indication of TPP-I spread, either through retrograde transport or by distribution through the CSF, will come from TPP-I-knock-out mice with a measurable and/or histological phenotype where issues of clearance of pathology relative to enzyme activity levels can be addressed.

The vectors used in this study resulted in a three- to seven-fold increase over endogenous TPP-I activity following a single injection, and TPP-I distribution increased from 10 days to 16 weeks in mice injected with FIVTPP-I. In AAV5 and FIV, two vectors known to provide long-term expression, these levels were maintained until the end of the experiment at 10 and 33 weeks respectively. The levels of TPP-I activity required for

therapeutic benefit are currently unknown. Using other lysosomal disorders as a benchmark, generally 1–5% normal enzymatic levels are sufficient for beneficial effects by enzyme replacement therapies.^{23–25} Again, therapeutic levels of TPP-I that are undetectable by IHC or enzyme assay, may be sufficient for correction of the cellular phenotype, as seen in the mucopolysaccharidosis type VII mouse model.^{13,16,26}

Increased β-galactosidase activity in the region 5 mm caudal to the injection site in AdTPP-I-injected mice did not result in detectable local increases in TPP-I activity (Figure 5a). These cells were presumably infected at their termini followed by retrograde transport of the vector, leading to increased β-galactosidase activity. Lack of detectable TPP-I in these same cells could be due to assay sensitivity limits. An alternative possibility is that TPP-I was made in these cells with most anterogradely transported back to the injection site.

Injection of adenovirus into the cerebellum gave the most convincing evidence of secretion and uptake of TPP-I. Cells of the choroid plexus were very positive for TPP-I immunoreactivity but displayed no detectable β-galactosidase activity. Interestingly, expression of TPP-I in Bergman glia did not lead to TPP-I immunoreactivity in Purkinje cells. This may indicate that either Bergman glia do not secrete TPP-I, or that the nearby Purkinje cell soma and its extensive dendritic tree do not efficiently endocytose TPP-I.

In summary, the total distribution of TPP-I is the product of the intrinsic ability of the vector to spread from the injection site and the subsequent spread of the secreted gene product. Optimization of the efficiency of TPP-I delivery will require the use of vectors that demonstrate wide distribution and long-term expression. In addition, modifications of the secreted proteins may be employed to increase their ability to spread throughout the parenchyma.¹³ Maximizing distribution of the vectors or the specific gene product will facilitate effective therapies for LINCL and other lysosomal storage diseases.

Materials and methods

Viral constructs

An adenovirus encoding TPP-I in the E1 region was generated by sub-cloning the human TPP-I cDNA¹² into the pacAd5CMV plasmid. The resulting shuttle (Ad5CMVTPP-I) was recombined with pacAd5 9.2-100 in HEK 293 cells to produce recombinant adenovirus particles, AdTTP-I.²⁷ The second adenovirus used in this study contained a nuclear targeted lacZ (nlsβgal) sub-cloned into the E3 region in addition to TPP-I in E1. To generate this construct, the existing pacAd5 9.2-100 plasmid was modified to include a SmaI restriction site after deleting the E3 region.¹³ DNA containing nlsβgal was cut from the plasmid pAdCMVnlsβgal with PmeI and SpeI and sub-cloned into the pAd5E3RSV recombination shuttle. Ad5E3RSVnlsβgal was cut with SmaI and Ad5 9.2-100SmaI with SmaI and recombined using methods described earlier.^{13,28} The resulting plasmid pacAd5 9.2-100nlsβgal was then transfected with the Ad5CMVTPP-I shuttle in HEK 293 cells to make the dual-expressing virus Ad5TPP-I/nlsβgal.²⁷ Adenoviruses were purified by the University of Iowa Gene

Transfer Vector Core by CsCl gradient purification and titered by plaque assay on A549 and HEK 293 cells.

For FIV constructs, the TPP-I cDNA was cloned into the pVETLRSVmc5 FIV genome plasmid.²⁹ The TPP-I-containing plasmid was combined with pCFIV Δ orf Δ vif and pCMV-G in a triple transfection in HT 1080 cells.^{19,29} The medium was collected over a 4-day period, passed through a 0.45 μ M filter and centrifuged at 7500 g to concentrate the retrovirus particles. The pellet was then resuspended in 1 mL lactose buffer (40 mg/ml lactose in PBS). Viral titers of FIVTPP-I were estimated by infecting A549 cells with serial dilutions of the viral stock followed by immunohistochemistry for TPP-I. FIV particles were generated in the University of Iowa Gene Transfer Vector Core.

Recombinant AAV5 vectors were produced by triple transfection of the TPP-I expression cassette, containing the native AAV5 ITR and the Rous Sarcoma virus long terminal repeat promoter, a plasmid containing AAV5 rep and cap, and a third plasmid containing helper function from adenovirus type 5. Recombinant AAV5TPP-I was purified as described previously and titered by quantitative PCR.^{20,30,31} The viral titer was 1.0×10^{12} genome copies (particles)/ml. AAV5TPP-I was dialyzed against lactated Ringer's solution prior to injection.

Animals and injections

Six-week-old C57Bl/6 mice were purchased from Jackson Labs (Bar Harbor, ME, USA) and housed at the University of Iowa Animal Care Facility. The University of Iowa Animal Care and Use Committee approved all animal procedures. For striatal injections, mice were injected at coordinates 0.4 mm rostral, 2 mm lateral from the bregma, at a depth of 3 mm with 5 μ l injections of one of the following viruses: 7.0×10^7 i.u. of AdTPP-I/nls β gal ($n=12$), 2.5×10^6 i.u. of FIVTPP-I ($n=14$) or 5×10^9 pt of AAV5TPP-I ($n=6$). For cerebellar injections, 2 μ l of virus containing 2.8×10^9 i.u. of AdTPP-I/nls β gal ($n=3$) or 1×10^6 i.u. of FIVTPP-I ($n=3$) was injected into the anterior cerebellar lobe underlying the midline posterior occipital bone using a Hamilton syringe cemented with a glass micropipette tip.²⁰ Control animals either received no injection ($n=4$), or were injected with Ad5nls β gal ($n=4$).

Tissue harvest and processing

All animals injected with adenovirus and FIV were evaluated 10 days after injection ($n=6$ each) and AAV5 animals at 10 weeks ($n=5$). Mice injected with FIV animals were also evaluated at 16 weeks ($n=4$) and 33 weeks ($n=3$).

For cryostat sections and immunohistochemistry, animals were perfused with 2% paraformaldehyde. Brains were removed and post-fixed 2 h in 2% paraformaldehyde, cryoprotected overnight in 30% sucrose, embedded in OCT and sectioned on a cryostat at 10 μ m for subsequent immunostaining.

For enzyme assays, mice were euthanized and the brains removed, cut rostral to caudal at 1 mm intervals and hemispheres separated for analysis. Samples were frozen immediately in liquid N₂ and extracts prepared by homogenization in 500 μ l of ice-cold lysis buffer (0.15 M NaCl, 0.1% Triton X-100). Nuclei and cellular debris were pelleted at 10 000 g at 4°C. The soluble fraction was removed and saved for TPP-I analysis.

Nuclear pellets from Ad-injected mice were retained for β -galactosidase activity and were sonicated for 10 s in 500 μ l of lysis solution. All samples were frozen at -80°C until assayed. Protein concentrations were determined by the DC protein assay (BioRad, Hercules, CA, USA).

TPP-I antibody and immunohistochemistry

Antibodies against TPP-I were generated by injecting rabbits with 500 μ l of 1×10^{12} pt/ml of AdTPP-I into four intramuscular and one intradermal site. The rabbits were boosted with the same dosage and routes 2 weeks later. Serum aliquots were stored at -20°C . Rabbit serum was tested for TPP-I specific antibodies by immunostaining (1) transfected cells containing expression plasmids devoid of all adenovirus sequences, (2) cells infected with FIVTPP-I, and (3) tissue sections from mice injected with adenovirus expressing human β -glucuronidase and nuclear-targeted β -galactosidase (Ad β gluc/nls β gal). Antibodies directed against TPP-I were detected in TPP-I-expressing tissues and cells but not in Ad β gluc/nls β gal-injected mice. Rabbit anti-TPP-I serum was used at 1:600. To detect neurons, mouse anti-NeuN 1:100 (Chemicon International Inc., Temecula, CA, USA) directly conjugated to Alexa 568 (Molecular Probes, Eugene, OR, USA) was used. Polyclonal rabbit anti- β -galactosidase (BioDesign International, Sao, MN, USA), directly conjugated to Alexa 568 and diluted 1:1500 was used to detect cells infected with adenovirus. All antibodies were diluted in 3% BSA, 0.1% saponin, 0.3% Triton X-100 in PBS (diluent). After blocking tissue sections for 30 min in diluent containing 10% serum, samples were incubated with primary antibodies overnight at 4°C. Samples were washed extensively in diluent and stained with fluorescently labeled secondary antibodies for 2 h at room temperature. Photomicrographs were captured using Adobe Photoshop and a SPOT/RT digital camera (Diagnostic Inst, Sterling Heights, MI, USA) on a Leica DMRBE fluorescent microscope or Olympus IX70 inverted microscope.

LINCL fibroblasts

LINCL fibroblasts previously isolated from patients were kindly provided by Dr Peter Lobel (Rutgers University, Piscataway, NJ, USA). Compound heterozygous fibroblasts that contained a G3560C splice junction mutation and a C3674T non-sense mutation in *TPP-I* were used to evaluate the ability of these deficient cells to sequester and activate TPP-I expressed from viral vectors. Fibroblasts were grown in DMEM supplemented with 10% FCS plus pen/strep. Fibroblasts were cultured in media containing 2% FCS, DMEM and 10 MOI of AdTPP-I/nls β gal added for 4 h, followed by removal of virus. Cells were cultured for an additional 48 h before TPP-I activity assays were done on media and cell lysate fractions. To test for TPP-I uptake, A549 cells were infected at an MOI of 50 in DMEM containing 2% FCS, DMEM for 4 h, followed by virus removal and an additional 48 h culture. The medium was removed 48 h after infection and added to patient fibroblast cultures in six-well plates. Media and cells were harvested and TPP-I activity measured. For immunohistochemistry, patient cells were cultured for 48 h in TPP-I-enriched media harvested from virally infected A549 cells and then stained with anti-TPP-I.

Enzyme activity assays

β -Galactosidase and TPP-I enzyme activities were analyzed in a 96-well fluorescence microplate reader (BMG Technologies, Durham, NC, USA) with Costar 3631 plates (Fisher Scientific, Pittsburgh, PA, USA). TPP-I activity was measured at 37°C using the substrate Ala-Ala-Phe 7-amido-4-methylcoumarin (AAF-AMC; Sigma St. Louis, MO, USA) at 380 nm excitation, 460 nm emission.³² Prior to assay, samples were either maintained at neutral pH or pre-activated by incubation in citrate buffer (0.15 M NaCl, 0.05 M sodium citrate pH 4.2) for 20 min. Plates were pre-warmed to 37°C prior to the addition of substrate (50 μ l of 400 μ M AAF-AMC in citrate buffer). Samples were read every 2 min for 30 min. TPP-I activities from all mice were expressed as fluorescent units per minute per mg protein. Endogenous TPP-I activities from non-injected control mice were used to determine fold increase in expression after viral injections.

β -Galactosidase activities were measured in the nuclear fraction of all adenovirus-injected mice using the FluoReporter *lacZ* Quantitation Kit (Molecular Probes, Eugene, OR, USA) in accordance with the manufacturer's directions. Standard curves were generated using 0.02–5 ng purified β -galactosidase (Sigma, St. Louis, MO, USA). Aliquots of 5 μ l of nuclear extract or β -galactosidase were incubated with 1.1 mM 3-carboxy-umbelliferyl β -D-galactopyranoside in reaction buffer (0.1 M sodium phosphate, pH 7.3, 1 mM magnesium chloride and 45 mM β -mercaptoethanol) for 30 min at room temperature. Stop buffer (0.2 M Na₂CO₃) was added and the fluorescent product measured at 380 nm excitation and 460 nm emission. Emission values were converted to pg β -galactosidase per mg protein based on β -galactosidase standard curves and sample protein concentrations.

Acknowledgements

The authors thank Dr Istvan Sohar and Dr Peter Lobel for assistance with the TPP-I activity assays, Dr Sybille Sauter for the FIVTPP plasmid, Inês Martins and Ken Ratliff for excellent technical assistance and Drs Colleen Stein and Jason Heth for critical discussions. We also thank the University of Iowa Gene Transfer Vector Core (DK 54759) for help with virus production. This work was supported in part by a grant from the Batten Disease Support and Research Association (BDSRA), and from the Roy J. Carver Trust (BLD).

References

- 1 Opitz JM. *Ceroid-lipofuscinoses. Batten Disease and Allied Disorders*. Alan R. Liss, Inc.: New York, 1987, pp 1–307.
- 2 Goebel HH, Mole SE, Lake BD. *The Neuronal Ceroid Lipofuscinoses (Batten Disease): Biomedical and Health Research*. IOS Press: Amsterdam, 1999, p 33.
- 3 Sohar I, Sleat DE, Jadot M, Lobel P. Biochemical characterization of a lysosomal protease deficient in classical late infantile neuronal ceroid lipofuscinosis (LINCL) and development of an enzyme-based assay for diagnosis and exclusion of LINCL in human specimens and animal models. *J Neurochem* 1999; **73**: 700–711.

- 4 Palmer DN *et al*. Mitochondrial ATP synthase subunit c storage in the ceroid-lipofuscinoses (Batten disease). *Am J Med Genet* 1992; **42**: 561–567.
- 5 Sleat DE *et al*. Association of mutations in a lysosomal protein with classical late-infantile neuronal ceroid lipofuscinosis. *Science* 1997; **277**: 1802–1805.
- 6 Vines D, Warburton MJ. Purification and characterisation of a tripeptidyl aminopeptidase I from rat spleen. *Biochim Biophys Acta* 1998; **1384**: 233–242.
- 7 Rawlings ND, Barrett AJ. Tripeptidyl-peptidase I is apparently the CLN2 protein absent in classical late-infantile neuronal ceroid lipofuscinosis. *Biochim Biophys Acta* 1999; **1429**: 496–500.
- 8 Vines DJ, Warburton MJ. Classical late infantile neuronal ceroid lipofuscinosis fibroblasts are deficient in lysosomal tripeptidyl peptidase I. *FEBS Lett* 1999; **443**: 131–135.
- 9 Lin L, Sohar I, Lackland H, Lobel P. The human CLN2 protein/tripeptidyl-peptidase I is a serine protease that autoactivates at acidic pH. *J Biol Chem* 2001; **276**: 2249–2255.
- 10 Ezaki J, Takeda-Ezaki M, Kominami E. Tripeptidyl peptidase I, the late infantile neuronal ceroid lipofuscinosis gene product, initiates the lysosomal degradation of subunit c of ATP synthase. *J Biochem* 2000; **128**: 509–516.
- 11 Ezaki J, Tanida I, Kanehagi N, Kominami E. A lysosomal proteinase, the late infantile neuronal ceroid lipofuscinosis gene (CLN2) product, is essential for degradation of a hydrophobic protein, the subunit c of ATP synthase. *J Neurochem* 1999; **72**: 2573–2582.
- 12 Lin L, Lobel P. Production and characterization of recombinant human CLN2 protein for enzyme-replacement therapy in late infantile neuronal ceroid lipofus. *Biochem J* 2001; **357**: 49–55.
- 13 Xia H, Mao Q, Davidson BL. The HIV Tat protein transduction domain improves the biodistribution of β -glucuronidase expressed from recombinant viral vectors. *Nat Biotechnol* 2001; **19**: 640–644.
- 14 Consiglio A *et al*. *In vivo* gene therapy of metachromatic leukodystrophy by lentiviral vectors: correction of neuropathology and protection against learning impairments in affected mice. *Nat Med* 2001; **7**: 310–316.
- 15 Ghodsi A *et al*. Extensive β -glucuronidase activity in murine CNS after adenovirus mediated gene transfer to brain. *Hum Gene Ther* 1998; **9**: 2331–2340.
- 16 Stein CS, Ghodsi A, Derksen T, Davidson BL. Systemic and central nervous system correction of lysosomal storage in mucopolysaccharidosis type VII mice. *J Virol* 1999; **73**: 3424–3429.
- 17 Vogler C *et al*. Murine mucopolysaccharidosis type VII: the impact of therapies on the clinical course and pathology in a murine model of lysosomal storage disease. *J Inherit Metab Dis* 1998; **21**: 575–586.
- 18 Bosch A *et al*. Reversal of pathology in the entire brain of mucopolysaccharidosis type VII mice after lentivirus-mediated gene transfer. *Hum Gene Ther* 2000; **11**: 1139–1150.
- 19 Brooks AI *et al*. Functional correction of established CNS deficits in an animal model of lysosomal storage disease using feline immunodeficiency virus-based vectors. *Proc Natl Acad Sci USA* 2002; **99**: 6216–6221.
- 20 Alisky JM *et al*. Transduction of murine cerebellar neurons with recombinant FIV and AAV5 vectors. *NeuroReport* 2000; **11**: 2669–2673.
- 21 Davidson BL *et al*. Recombinant AAV type 2, 4, and 5 vectors: transduction of variant cell types and regions in the mammalian CNS. *Proc Natl Acad Sci USA* 2000; **97**: 3428–3432.
- 22 Fu H *et al*. Neurological correction of lysosomal storage in a mucopolysaccharidosis IIIB mouse model by adeno-associated virus-mediated gene delivery. *Mol Ther* 2002; **5**: 42–49.
- 23 Barranger JA, O'Rourke E. Lessons learned from the development of enzyme therapy for Gaucher disease. *J Inherit Metab Dis* 2001; **24**: 89–96.

- 24 Desnick RJ, Banikazemi M, Wasserstein M. Enzyme replacement therapy for Fabry disease, an inherited nephropathy. *Clin Nephrol* 2002; **57**: 1–8.
- 25 Leone P, Janson CG, McPhee SJ, During MJ. Global CNS gene transfer for a childhood neurogenetic enzyme deficiency: Canavan disease. *Curr Opin Mol Ther* 1999; **1**: 487–492.
- 26 Ghodsi A *et al*. Systemic hyperosmolality improves β -glucuronidase distribution and pathology in murine MPS VII brain following intraventricular gene transfer. *Exp Neurol* 1999; **160**: 109–116.
- 27 Anderson RD *et al*. A simple method for the rapid generation of recombinant adenovirus vectors. *Gene Ther* 2000; **7**: 1034–1038.
- 28 Chartier C *et al*. Efficient generation of recombinant adenovirus vectors by homologous recombination in *Escherichia coli*. *J Virol* 1996; **70**: 4805–4810.
- 29 Johnston JC *et al*. Minimum requirements for efficient transduction of dividing and nondividing cells by feline immunodeficiency virus vectors. *J Virol* 1999; **73**: 4991–5000.
- 30 Chiorini JA *et al*. High-efficiency transfer of the T cell co-stimulatory molecule B7-2 to lymphoid cells using high-titer recombinant adeno-associated virus vectors. *Hum Gene Ther* 1995; **6**: 1531–1541.
- 31 Davidson BL, Chiorini JA. Recombinant adeno-associated virus vector types 4 and 5: preparation and application for CNS gene transfer. *Viral Vectors Gene Ther* 2003 (in press).
- 32 Page AE, Fuller K, Chambers TJ, Warburton MJ. Purification and characterization of a tripeptidyl peptidase I from human osteoclastomas: evidence for its role in bone resorption. *Arch Biochem Biophys* 1993; **306**: 354–359.